Materials Science Forum Vols. 738-739 (2013) pp 496-500
Online available since 2013/Jan/25 at www.scientific.net
© (2013) Trans Tech Publications, Switzerland
doi:10.4028/www.scientific.net/MSF.738-739.496

Shape Memory Properties of Ultrafine-Grained Austenitic Stainless Steel

Karine Andrea Käfer[1,a], Heide Heloise Bernardi[1,b],
Leonardo Kenji Fudo Naito[1,c], Nelson Batista de Lima[2,d], Jorge Otubo[1,e]

[1]Instituto Tecnologico de Aeronautica, S. J. Campos, Brazil.

[2]Instituto de Pesquisas Energeticas e Nucleares, Sao Paulo, Brazil.

[a]karine@ita.br, [b]heide@ita.br, [c]lnaito@ita.br, [d]nblima@ipen.br, [e]jotubo@ita.br

Keywords: Shape Memory Alloy, ECAE, Grain size, Compression tests.

Abstract. In this work the effect of grain refinement on the shape memory properties of a Fe-Mn-Si-Cr-Ni-Co-Ti alloy was evaluated using compression tests. In order to refine the microstructure, the samples were heavily deformed by Equal Channel Angular Extrusion (ECAE) and then annealed at different temperatures ranging from 723 K to 1323 K. These treatments resulted in the formation of intermetallic precipitates and strengthening of austenitic matrix. The results of compression tests show that the higher degrees of shape recovery (56 % for 4% strain) were achieved by the samples with smaller grain size (12 μm). It was also shown that the contribution of elastic shape recovery increases and the shape recovery due memory effect decreases as the austenitic matrix strengthening increases.

Introduction

Stainless shape memory steels were first developed during 1990s [1], and since then, they have been studied for a variety of applications. This class of materials exhibit advantageous characteristics like good corrosion resistance, good mechanical properties and low cost but with lower shape recovery compared to NiTi, limiting their widespread use in engineering [2]. These alloys possess a microstructure comprising primary austenite and some amount of thermal martensite. The parent austenite phase γ (FCC) is susceptible to a non-thermoelastic transformation to hexagonal ε (HC) martensite, during the prestraining. Reversion of this ε martensite by heating promotes the shape recovery [3].

Recent studies [2, 4] show that the lower shape memory properties of polycrystalline alloys are caused mostly by inter-granular constraints, like the concurrent dislocation glide or the irreversibility of phase transformation. In particular, the intersection of ε martensite plates during the deformation process is reported as one of the main reasons for incomplete shape recovery [4]. Yang and co-workers [5] observed that during the deformation process, intersections of martensite plates could promote the strain-induced nucleation of α′ (BCC) martensite and strain-hardening effect opposing deformation. Under these conditions, the forward transformation dislocations cannot make the backward movement, reducing the transformation reversibility [4]. Thus, to improve the shape memory effect, the martensite plates should be formed in domains with a single variant, avoiding collisions between the plates belonging to different orientations.

The grain refinement can be an alternative to produce monovariant martensite plates and increase the strength of austenitic parent phase, suppressing permanent slip. According to Otubo et al. [1] in large grain size more than one variant needs to be activated to accommodate the shear strain generated during the martensitic transformation.

Based on these works, the present study aims to investigate the effect of grain refinement on shape memory properties of a Fe-Mn-Si-Cr-Ni-Co-Ti alloy processed by Equal Channel Angular Extrusion (ECAE) technique. In the current work, 0.4 wt.% Ti was used to improve the mechanical properties of austenitic matrix. Considering that titanium presents a high reactivity, it is also expected the formation of intermetallic precipitates in grain boundaries. This precipitates could avoid the grain growth during subsequent annealing treatments [6].

All rights reserved. No part of contents of this paper may be reproduced or transmitted in any form or by any means without the written permission of TTP, www.ttp.net. (ID: 143.107.255.190, University of Sao Paulo, SAO PAULO - SP, Brazil-04/08/14,15:22:53)

Experimental

The stainless shape memory alloys used in this work was produced by conventional vacuum induction melting (VIM). The nominal composition of the alloy is Fe-7.4Mn-4.6Si-13.12Cr-6.35Ni-12.18Co-0.4Ti-0.03C (in wt.%). The ingot of 65 x 65 mm² was heated at 1473 K for 2 h, hot forged into bars of 40 x 40 mm² and longitudinally sectioned into 20 x 20 mm² bars. These bars were heated to 1323 K for 0.5h and hot rolled to 80 x 16 x 8 mm plates. To be processed through ECAE the plates were machined into 7 x 7 x 70 mm bars, solution treated at 1323 K for 1 h and then quenched into water.

The samples were extruded in an ECAE die with rectangular channel of 7 x 7 mm^2 and internal die angle of 120°. First, the samples were coated by copper based lubricant, introduced into the channel and then taken to an environmental chamber coupled to Instron Testing Machine. The environmental chamber was heated to 523 K, and after the temperature stabilization, the bar was pressed through the die at a speed of 5 mm/min. One set of samples were processed with 2 ECAE passes. In this case, after the first extrusion, the bars were rotated by 90° about the longitudinal axis, and extruded once more. The ECAE processed samples were cut in several parts, and then, each part was annealed for 1 h at different temperatures ranging from 723 K to 1323 K.

The corresponding microstructures and chemical microanalysis of constituents were examined using Jeol-5900 LV scanning electron microscope (SEM) equipped with an energy dispersive spectrometer (EDS) system. The lattice parameters were determined by a Rigaku Multiflex X-ray diffractometer, using Cu K_α radiation. The hardness measurements of samples were made in a Vickers hardness tester (Future-Tech FM-700) with a load of 200 g in order to determine the recrystallization temperature. Mechanical properties were evaluated by compression tests performed in an Instron Test Machine. The grain size was calculated in the cross section of the specimens in transversal directions (TD) and normal direction (ND) related to extrusion direction using the standard test method ASTM E112.

Results and Discussion

The Fig. 1 shows the effects of ECAE processing and annealing temperatures on the microstructure of a Fe-Mn-Si-Cr-Ni-Co-Ti alloy. Before processing, all the samples were solution treated (ST) at 1323 K/1h (Fig 1a). In this condition, the microstructure is essentially composed by equiaxed austenitic grains within stacks of thin martensite plates, annealing twins and a number of large precipitates. These precipitates were located mainly at the triple junction and grain boundaries. The EDS analysis showed that the precipitates were enriched in Ti, Cr and Si, with complementary changes in austenitic phase. The results are presented in Table 1, and the precipitates are referred as primary precipitates (P_1). These particles did not change size and morphology with further processing and heat treatments. As a reference, the ingot initial composition is shown in Table 1.

Table 1 – Chemical compositions of the constituent phases [wt.%].

Constituent	Si	Ti	Cr	Mn	Co	Ni	Fe
Ingot	4.60	0.40	13.12	7.40	12.18	6.35	55.95
Primary Precipitates (P_1)	9.14	3.64	16.28	7.59	12.37	5.65	45.00
Secondary Precipitates (P_2)	6.41	0.23	15.06	8.09	12.32	6.32	51.57

Fig. 1b shows the micrograph of a specimen submitted to 2 ECAE passes. The deformed grains present some amount of stress induced martensite plates and shear bands. After processing, the samples were subjected to heat treatments in different temperatures, in order to verify the microstructural evolution and grain refinement. The annealing treatments performed at 723 K and 823 K resulted in no significant changes in the microstructure and they are not shown. As observed in Fig. 1c, the samples treated at 923 K/1h presented the formation of new grains and precipitation of small particles. It was also in this condition that the smaller grain size was found for both samples, processed with 1 ECAE pass (20 μm) and 2 ECAE passes (12 μm), indicating that the recrystallization occurred in this range of temperature. Increasing the annealing temperature to 1023 K /1h (Fig. 1d) promoted an increment in precipitation rate. These precipitates grew coarser in subsequent higher annealing temperatures and they changed from irregular morphology (Fig. 1e) to spherical one (Fig. 1f) The EDS analysis (Table 1) showed that those precipitates, referred as secondary precipitates (P_2), were depleted in Fe, and enriched in Si and Cr.

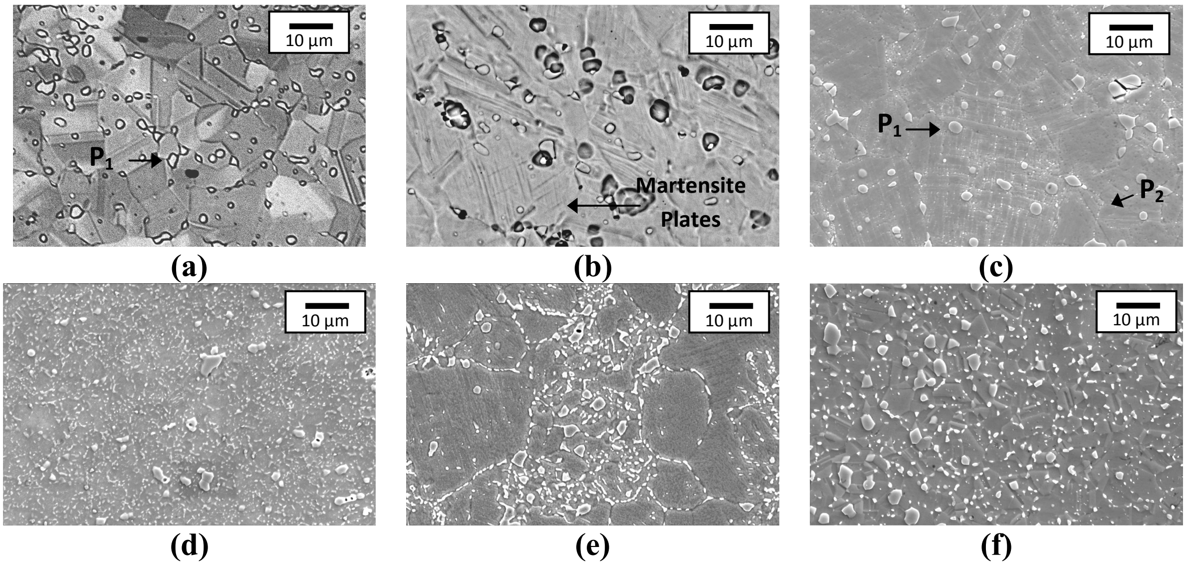

Fig. 1. Microstructures of the samples at different stages of processing (TD-ND): (a) Solution treated (ST), (b) ST + 2 ECAE passes (SEM-BSE); (c) ST + 2 ECAE + 923 K/1h, (d) ST + 2 ECAE + 1023 K/1h, (e) ST + 2 ECAE + 1123 K/1h, (f) ST + 2 ECAE + 1223 K/1h (SEM-SE).

X-Ray diffraction (XRD) was used to identify the phases present in the samples. The results are shown in Fig. 2. The XRD peaks of solution treated sample indicate the presence of both γ austenite and ε martensite in the microstructure. It was also observed 4 peaks assigned to the primary precipitates (P_1). These peaks were used to estimate the crystal structure and lattice parameter of the precipitate. It was found that the primary precipitates present a FCC structure and a lattice parameter of 0.407 nm. The diffractogram of sample processed in ECAE and annealed at 1023 K (Fig. 2b) also shows peaks relating to austenite and martensite. Besides, it is found that this sample has a higher volume fraction of ε martensite than solution treated by comparing the ε (10.0) and ε (10.1) peaks. The peaks attributed to the primary precipitates (P_1) did not change the intensity, indicating that this phase remain unchanged by processing and heat treatment, in agreement with analysis of microstructure (Fig. 1). It was also observed the appearance of 5 different peaks assigned to secondary precipitates (P_2), but the crystal structure of the particles could not be identified.

The variation in hardness values as a function of processing stages and heat treatments is shown in Fig. 3. In the solution treated condition, the hardness of samples were about 250 HV and after the 1 ECAE pass the hardness increased to 315 HV and to almost 400 HV for 2 ECAE passes. Those hardness increases are related to work hardening. Corroborating with micrographs shown in Fig. 1, the heat treatments ranging from 723 K to 1023 K caused the precipitation hardening of austenitic matrix, resulting in significant increase in hardness values. This effect is more evident for samples processed with 2 ECAE passes. The maximum value of 502 HV was achieved for sample deformed and annealed at 923 K. This strengthening effect occurs because during severe plastic deformation, high densities of dislocations are generated in the microstructure decreasing the activation energy for nucleation of precipitates, resulting in higher amount of precipitates in the microstructure [6].

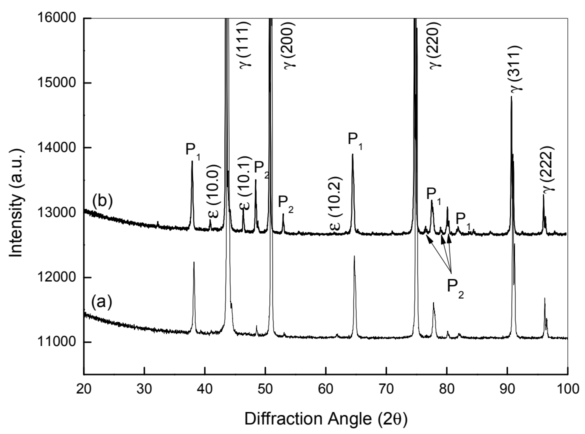

Fig. 2. XRD spectra for: (a) ST sample, (b) ST + 2 ECAE passes +1023 K.

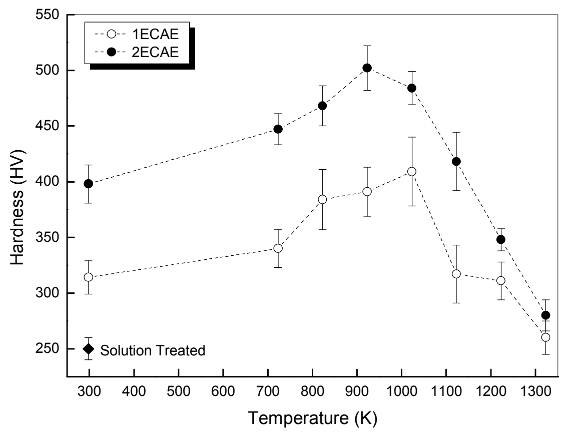

Fig. 3. Effect of annealing temperature on hardness of samples processed by 1 and 2 ECAE passes.

The Fig. 4 shows the effects of aging temperature and grain size on degree of shape recovery for samples processed with 1 and 2 ECAE passes. Initially, at solution treated state, the values of shape recovery capability were not expressive, around 40% for 4% strain. However, after extrusion and subsequent annealing the shape recovery capability improved. The maximum values were 52% and 56% total shape recovery after annealing at 923 K/1h, respectively for 1 ECAE and 2 ECAE passes samples. Coincidently, at this temperature, the samples present the smaller grain size, 20 μm for 1 ECAE pass and 12 μm for 2 ECAE passes. These results are in agreement with previous findings reported in the literature [1, 6], and demonstrate that the grain refinement is an important parameter to improve shape recovery. Nevertheless, the presence of second-phase particles in the microstructure also should be considered to explain the shape memory behavior.

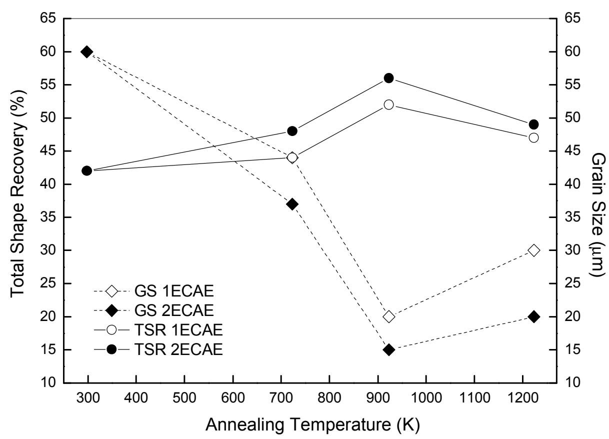

Fig. 4. Effect of annealing temperature on Grain Size (GS) and Total Shape Recovery (TSR) for ε = 4%.

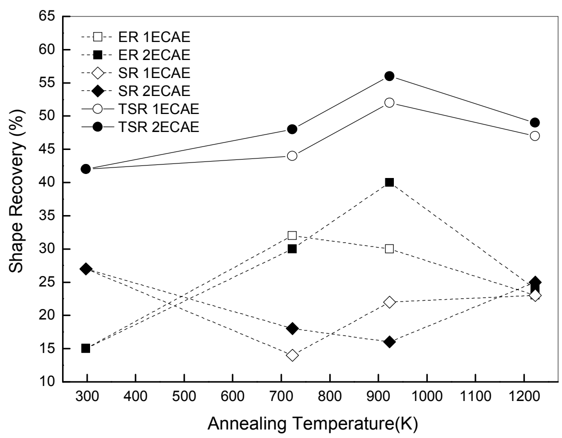

Fig. 5. Elastic Shape Recovery (ER), Shape Recovery (SR) and Total Shape Recovery (TSR) as a function of annealing temperature.

To evaluate the effect of second-phase particles, the total shape recovery (TSR) was separated in two parts: the elastic shape recovery (ER) obtained upon unloading the compressed sample and the shape recovery due to memory effect (SR) upon annealing at 873 K / 30 min.

As shown in Fig. 5, the main contribution to total shape recovery for solution treated sample is the shape memory effect, around 28% and the contribution due to elastic recovery is around 15% given a total shape recovery of 43%. After extrusion and annealing, the elastic recovery contribution surpasses the recovery due to shape memory being around 33% for 1 ECAE pass and 40% for 2 ECAE passes. The only difference is that the maximum elastic shape recovery for 1 ECAE pass happens at annealing temperature of 723 K while for 2 ECAE passes, the maximum is located at 923 K. The shape recoveries due to shape memory effect are minimum at these same temperatures. Increasing the annealing temperature to 1223 K, the contribution of elastic shape recovery decreases and contribution due to shape memory increases converging to the same values. For 1 ECAE pass sample, the grain size is the key factor for the improvement of total shape recovery degree. In this case, the best shape recovery was achieved in the recrystallization temperature (923 K) due to the formation of defect-free new grains. As previously discussed, for 1 ECAE pass, the precipitation was not high, and the particles were located mainly at the grain boundaries. For 2 ECAE passes, the precipitates density was considerably increased, resulting in strengthening of austenitic matrix. In this case, the precipitates could hinder the movement of Shockley partial dislocation, reducing the shape recovery due to shape memory and increasing the elastic shape recovery. For higher annealing temperature, the precipitates start to coalesce, the matrix strengthening mechanism decreases and the contribution of shape memory effect to the total shape recovery increases concomitantly decreasing the elastic shape recovery. This elastic shape recovery could be called superelastic shape recovery.

Conclusions

This study has examined the microstructure, mechanical properties, and shape memory performance of Fe-Mn-Si-Cr-Ni-Co-Ti alloy after ECAE processing. It has been concluded that annealing treatments performed in temperature range from 723 K to 1023 K results in precipitation of second-phase particles and grain refinement. The particles precipitation promotes the strengthening of austenitic matrix, resulting in increase of hardness values. The best shape recovery performance was 52% and 56%, respectively for samples processed with 1 and 2 ECAE passes, and annealed at 923 K. For 1 ECAE pass, the maximum value of shape recovery is related to the recrystallization mechanism, resulting in formation of defect-free new grains. For 2 ECAE passes, the main factor was the increase of elastic recovery caused by the high density of precipitates.

Acknowledgements

Authors are thankful to FAPESP (Grants n^o 00/09730-1; 2009-09091-3; 2010/20565-4), CNPq Universal (Grant n^o 473612/2006-2), CNPq Casadinho - UFCG/ITA, FINEP/PRO-INFRA, Villares Metals SA, IEAv and ABTLus/LNLS.

References

[1] J. Otubo, F.C. Nascimento, P. R. Mei, L.P. Cardoso, M. J. Kaufman, Influence of grain austenite grain size on mechanical properties of stainless SMA. Mater. Trans. JIM. 43-5 (2002) 916-919.

[2] S. Kajiwara, Characteristics features of shape memory effect and related transformation behavior in Fe-based alloys. Mater. Sci. Eng. A 273-275 (1999) 67-88.

[3] S. M. Abbasi, A. Shokufar, Improvement of mechanical properties of Cr-Ni-Mo-Cu-Ti stainless steel with addition of vanadium. J. Iron and Steel. 14(6) (2007) 74-78.

[4] X. Min, T. Sawaguchi, X. Zhang, K. Tsuzaki, Reasons for incomplete shape memory recovery in polycrystalline Fe-Mn-Si shape memory alloys. Scripta. Mater. 67 (2012) 37-40.

[5] J.H. Yang, C.M. Wayman, On secondary variants formed at intersections of ε martensite variants. Acta. Metall. Mater. 40 (1992) 2011-2023.

[6] W. Zhang, N. Li, Y. Wen, Microstructure and shape memory effect of different carbon-bearing FeMnSiCrNi alloys aged after equal channel angular pressing. Metall. Mater. Trans. B 38 (2007) 299-303.

European Symposium on Martensitic Transformations
10.4028/www.scientific.net/MSF.738-739

Shape Memory Properties of Ultrafine-Grained Austenitic Stainless Steel
10.4028/www.scientific.net/MSF.738-739.496

DOI References

[5] J.H. Yang, C.M. Wayman, On secondary variants formed at intersections of ε martensite variants. Acta. Metall. Mater. 40 (1992) 2011-(2023).
http://dx.doi.org/10.1016/0956-7151(92)90187-J